Effects of Axial Solvent Coordination to Dirhodium Complexes on Reactivity and Selectivity in C–H Insertion Reactions: A Computational Study

Croix J. Laconsay,[a] Anna Pla-Quintana,[a,b] and Dean J. Tantillo[a]*

[a]Department of Chemistry, University of California, Davis, CA 95616, United States

[b]Institut de Química Computacional i Catàlisi (IQCC) and Departament de Química, Universitat de Girona (UdG), Facultat de Ciències, C/Maria Aurèlia Capmany, 69, 17003-Girona, Catalunya, Spain

KEYWORDS

Dirhodium tetracarboxylate catalyst; C-H insertion; axial coordination; solvent effects; density functional theory

ABSTRACT

Density functional theory calculations were used to systematically explore the effects of axial ligation by solvent molecules on the reactivity and selectivity of dirhodium tetracarboxylates with diazo compounds in the context of C–H insertion into propane. Insertions on three types of diazo compounds—acceptor/acceptor, donor/acceptor, and donor/donor—promoted by dirhodium tetraformate were tested with and without axial solvent ligation for no surrounding solvent, dichloromethane, isopropanol, and

acetonitrile. Magnitudes, origins, and consequences of structural and electronic changes arising from axial ligation were characterized. The results suggest that axial ligation affects barriers for N_2 extrusion and C–H insertion, the former to a larger extent.

INTRODUCTION

Overview and historical context

Dirhodium tetracarboxylate complexes (Scheme 1, left) are among the most commonly used catalysts in organometallic chemistry. These bimetallic complexes have a "paddle wheel" (sometimes called "lantern") structure, containing a Rh–Rh single bond, the details of which has been subject to experimental and theoretical interrogations for decades.[1–8] These complexes—which have applications spanning from catalysis[9,10] and biology[11–13] to supramolecular chemistry[14–17]—are potent catalysts in organic chemistry because of their ability to promote nitrogen extrusion from diazo compounds to generate transient rhodium carbene intermediates (Scheme 1, center, L = CR_2). These intermediates are capable of engaging in a wide range of chemical reactions including (2 + 1) cycloadditions (e.g., cyclopropanation, cyclopropenation, insertion into X–H bonds), various (n + 1) cycloaddition reactions where n > 2, and a diverse array of ylide reactions.[18–27] The efficiency and selectivity imparted by dirhodium tetracarboxylate catalysts, including enantioselectivity when chiral carboxylate (or related) ligands are used, makes them especially useful tools in the construction of complex organic molecules.[28–30] While one of the two rhodium atoms is involved directly in bond-making/breaking with substrates,[31] the other is crucial for the overall catalytic performance of the complex, as it is involved in compensating for electronic alterations during a reaction (a phenomenon referred to as the *trans* effect or *trans* influence).[32,33]

Scheme 1. Dirhodium "paddlewheel" complexes have four bridging bidentate bridging ligands and two axial sites for additional ligands (L) to bind.

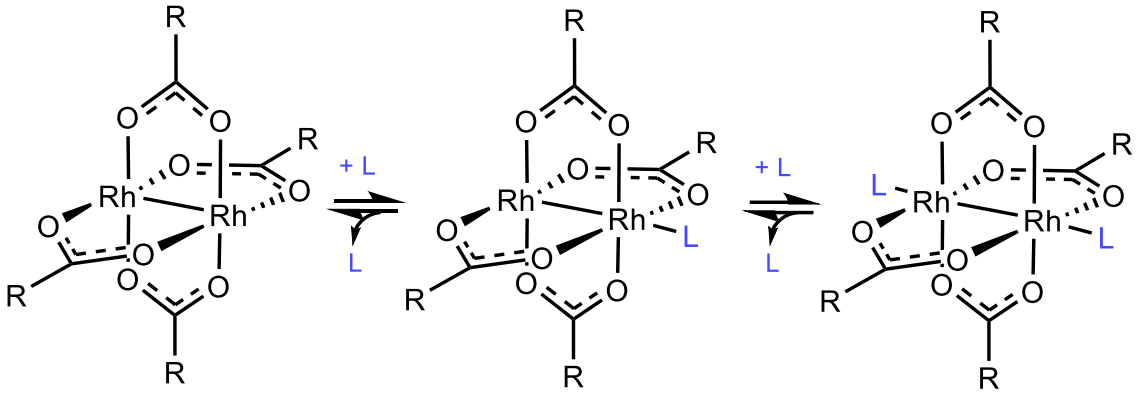

Each of the two rhodium atoms in a dirhodium tetracarboxylate is Lewis acidic and can complete an octahedral geometry by filling the coordination site along the axis of the Rh–Rh bond. In the bioinorganic realm, the availability of these labile axial sites is crucial for anti-tumor activity and DNA targeting.[34] In heterogenous catalysis, axial ligation to dirhodium(II) complexes has been used to immobilize complexes in silica (e.g., SBA-15) materials.[35,36] Davies et al., for example, used axial coordination of pyridine groups from polymeric resins as a means to reuse chiral dirhodium catalysts with low to no effect on catalyst activity.[37–40]

Most reported X-ray crystal structures of dirhodium complexes contain bound axial ligands, usually solvent but sometimes substrates, other ligands, or other complexes (i.e., in coordination polymers).[41–47] Even though dirhodium complexes have been known since the 1960s, it was not until 2002 that an X-ray crystal structure of a dirhodium complex *without* axial ligands was reported.[48] The few reported X-ray structures of dirhodium *carbenes* crystallize as coordination polymers: OMe or NMe_2 groups present in the carbene appendants coordinate to the rhodium not bearing the carbene carbon of

the next unit.[49,50] These complexes require CH_2Cl_2 and toluene to be stable in crystalline form and their unit cells contain highly disordered solvent molecules.[49]

In solution, axial solvent coordination to dirhodium complexes is well known,[51–55] and even macroscopically evident due to its effect on the electronic structure of the complex. Coordination by solvent molecules is comparatively much weaker than carboxylate coordination. Nevertheless, as a result of populating a vacant Rh–Rh σ* orbital upon coordination (by solvent or other ligands), one will observe in color changes.[56–59] Triple resonance NMR experiments confirmed that axial ligand coordination changes the chemical environment at the Rh nuclei, and the donor strength of a labile ligand is observed in ^{103}Rh chemical shift "deshielding".[60] Several directions have been explored to effect changes on dirhodium complexes by way of axial ligation, some of which are summarized below.

Axial Ligands

Berry's three-center/four-electron (3c/4e) bonding model in the Rh–Rh–CR_2 fragment (Scheme 1, center, L = CR_2) helps rationalize the diverse reactivity of dirhodium carbenes.[58] As a result of the communication between these three atoms, dirhodium carbene reactivity is potentially "tunable" by axial ligation opposite to the Rh–C bond, a possibility being actively investigated. For instance, many have designed dirhodium complexes with improved catalytic properties[54,61–65] by incorporating ligands with tethered axial donors (or ligands that shield the Rh core from axial coordination by external molecules[66]). However, this direction is still in its infancy compared to that of modifying electronic and steric properties of the bridging ligands.[7]

Some have explored *N*-heterocyclic carbenes (NHCs) as external axial coordinating ligands. In one example, Snyder et al. isolated a dirhodium carboxylate complex with tetramethylimidazolidene coordinated to the axial position in order to obtain a dirhodium carbene structure suitable for X-ray structure characterization.[67] No significant differences in activity or selectivity were found with and without the NHC, which led the authors to conclude that an equilibrium was taking place that furnishes dirhodium carbene free of axial ligand as the active catalyst. Subsequently, Gois et al. utilized *N*,*N*-(2,6-diisopropylphenyl)imidazolidene, a more sterically hindered NHC, and obtained dirhodium dicarboxylates with axially coordinated NHCs to showcase different reactivity and selectivity.[68] These complexes catalyzed C–H insertion reactions of diazo compounds at considerably slower rates than the compounds without axial ligation and with substantial differences in selectivity. These observations were attributed to a "push-pull" mechanism, in which an axial NHC causes a weakening of the R–C_{NHC} bond in the presence of a bound diazo compound ("pull"), and the NHC weakens the R=$C_{carbene}$ partial double bond in the dirhodium carbene complex ("push").[68]

Axial complexation of groups that are not as strong σ-donors as NHCs also have been explored. Darko et al., for example, reported a heteroleptic dirhodium complex that contained a bridging ligand with a tethered thioether that axially coordinates to rhodium.[69] Beneficial effects on the activity – and especially the selectivity – were observed upon using the heteroleptic complex as a catalyst for cyclopropanation. Further studies from the same group with mixed oxazolidinate/carboxylate dirhodium complexes confirmed the positive effect that the coordination of tethered thioether donors had on the catalytic activity of the complexes in Si–H insertion reactions and cyclopropanation reactions.[63,64] The authors argued that the enhanced selectivity they observed was related to an increase in the energy of the LUMO of the complex upon coordination of the axial ligand.[55]

Coordinating Lewis basic additives may also lead to divergent outcomes. For instance, Doyle and coworkers disclosed a dearomatizing formal [3+3]-cycloaddition of isoquinolinium/pyridinium methylides and enol diazoacetates whose chemo- and enantioselectivity depended on Lewis base additives.[70] The main difficulty in this strategy is to find a suitable concentration of the additive that favors mono-coordination over di-coordination, since the latter would render the catalytic system inactive (Scheme 1, center and right). Additives such as tetramethyl urea, Hünig's base, *N*,*N*-diethylaniline, 2,4,6-trimethylpyridine, $TfNH_2$, DMAP, and 2-chloropyridine also have been used to modulate the reactivity and selectivity of dirhodium tetracarboxylate complexes through axial coordination.[71–75]

Solvent Effects

Solvent effects can be crucial in catalysis.[76] The effects of axial coordination by solvent on Rh-carbene reactivity and selectivity should be considered, since it has been shown that reaction outcome can highly depend on the solvent.[26,77–79] Weakly Lewis basic and non-polar/low-polarity solvents, expected to be poorly coordinating, such as dichloromethane or hexane, are generally considered the most efficient reaction media for C–H functionalization.[29] Still, there are examples reported of C–H insertion[80,81] and cyclopropanation[82] reactions in water, a highly coordinating, polar solvent. Though acetonitrile (CH_3CN), another Lewis basic solvent, sometimes works poorly in Rh-catalyzed reactions,[83,84] it has been shown to be an effective solvent for others.[85] Predicting an optimal solvent is not always trivial. For example, in a Rh-catalyzed C(sp^3)–H amination, *t*BuCN was identified as the optimal solvent because the lifetime of $Rh_2(esp)_2$ was prolonged in *t*BuCN compared to that in acetonitrile or CH_2Cl_2.[86]

Computational studies exploring the effects of axial solvent coordination on reactivity and selectivity are sparse. Davies and coworkers investigated one case (see Figure 6 of their study) of axially coordinated acetone on a dirhodium tetraformate catalyzed cyclopropanation of styrene by methyl phenyldiazoacetate, a donor acceptor carbene (at the B3LYP/6-311G(2d,2p)[Rh-RSC+4f]//B3LYP/6-31G(d)[Rh-RSC+4f] level of theory).[87] Their results indicated that acetone coordination slows down the rate of nitrogen (N_2) extrusion (a barrier increase of 4.7 kcal mol^{-1}) and makes it less exothermic (ΔE = -3.1 kcal mol^{-1}) compared to that without acetone coordination (ΔE = -9.1 kcal mol^{-1}). This reactivity difference, captured by DFT calculations, better aligns with their experimental data.

Kisan and Sunoj reported a computational study (at the SMD($CHCl_3$)-M06/LANL2DZ[6-31G(d,p)]//B3LYP/LANL2DZ[6-31G(d)] level of theory) in which axial solvent ($CHCl_3$) coordination was shown to have minimal effects on all reaction steps except for the step responsible for the enantioselectivity in an asymmetric N–H insertion reaction with cooperative dual catalysts: a chiral SPINOL-phosphoric acid and a dirhodium tetracarboxylate.[88] In addition, axial coordination of the chiral SPINOL-phosphoric acid catalyst seemed to selectively stabilize the preferred transition state structure (TSS).[88] Additionally, with the exception of some experimental-computational studies wherein axial ligation is explicitly considered in the computational studies (and compared to the non-complexed states),[89–91] axial ligation is generally *not* considered in computational modeling of synthetically-relevant reactions (including our own work[92,93]).

Goals of this work

If, for the most part, axial solvent ligation is ignored in computational studies of dirhodium catalyzed reactions, we ask '*should it be*'? The aim of the present work is to systematically evaluate the effects that coordination of single solvent molecules at the axial sites of dirhodium complexes has on C–H insertion reactions. Two main questions were the focus of our attention: (1) Is there a meaningful difference in reactivity and selectivity for such reactions when an implicit molecule is axially coordinated? (2) Is it possible to rationally tune reactivity and selectivity by solvent? Our tool of choice for answering these questions is density functional theory (DFT), which has been used effectively to model related systems on many occasions.[94] For more information on approaches and caveats for modeling organometallic reactions see our recent review[94] and excellent reviews published by others.[95–103]

COMPUTATIONAL METHODS

DFT calculations were carried out with the *Gaussian 09* quantum chemistry package.[104] Stationary points were classified as either TSSs or minima on the potential energy surface (PES) by identification of one imaginary frequency for the former and the absence of imaginary frequencies for the latter. To confirm that TSSs are connected to particular minima, we employed intrinsic reaction coordinate (IRC calculations).[105–107] For geometry optimizations, we used the B3LYP[108] functional with the LANL2DZ[6-31G(d)] basis set, i.e., the LANL2DZ effective core potential (ECP)[109] for Rh and 6-31G(d) for all other atoms. Implicit solvent was treated with the conductor-like polarizable continuum model (CPCM).[110–112] Reported energies are from single points using CPCM with the M06[113] functional with a larger basis set, the SDD[114] ECP for Rh and the 6-311+G(d,p) basis set for all other atoms. Natural bond orbital (NBO) calculations were carried out in Gaussian with Gaussian NBO version 3.1.[115–118]

We and others have shown that the B3LYP functional is a reasonable choice for geometry optimizations of relatively small systems involving dirhodium carbenes.[95,98,119–122] In fact this level of theory provides good agreement with experiment for $\Delta H^{\ddagger}$ for N_2 extrusion, the step that contains the turnover-determining transition state,[123] for the reactions we describe below with the methyl diazoacetate-dirhodium formate adduct: we compute a $\Delta H^{\ddagger}$ = 15.1 kcal mol^{-1} with B3LYP/LANL2DZ[6-31G(d)] versus an experimental $\Delta H^{\ddagger}$ of 15.0 kcal mol^{-1} for dirhodium tetraacetate-catalyzed cyclopropanation of ethyl diazoacetetate and styrene,[124] which can also be compared with $\Delta H^{\ddagger}$ of 13.3 kcal mol^{-1} for N_2 extrusion from diazoketones by Pirrung and coworkers.[31] Additionally, we tested other functionals and ECP basis sets: M06,[113] M06L,[125] and MN15[126] functionals with either the LANL2DZ or SDD basis set. Tracking the variation of relative electronic energies with respect to level of theory led us to conclude that M06/SDD[6-311+G(d,p)], which predicted the N_2 extrusion $\Delta E^{\ddagger}$ for the reaction mentioned above to be 16.4 kcal mol^{-1},[124] afforded a reasonable compromise of accuracy and computational cost (see SI, Figure S3).[113] Optimized stationary points using dispersion-corrected B3LYP (i.e., B3LYP-D3(BJ))[127,128] had little to no effect on the relative free energies (see SI, Table S3). As a result of these tests, we utilized the M06/SDD[6-311+G(d,p)]//B3LYP/LANL2DZ[6-31G(d)] level of theory throughout this study. Similar levels of theory have been employed for DFT investigations of synthetically-relevant, Rh-catalyzed C–H insertions.[129,130] All computed structures are available on the ioChem-BD platform[131] and can be accessed *via* https://doi.org/10.19061/iochem-bd-6-111. Energies and lowest vibrational frequencies are summarized in the Supporting Information using the files names on the ioChem-BD database for ease of access.

RESULTS AND DISCUSSION

Overall Approach

For simplicity, we selected the C–H insertion of three representative diazo compounds **1a-c**—one each with acceptor/acceptor (A/A),[20,132,133] donor/acceptor (D/A),[21,22,28,134] and donor/donor (D/D)[25,27,135,136] substituents—into propane (**2**) catalyzed by the simplest dirhodium tetracarboxylate, dirhodium tetraformate ([Rh_2(formate)$_4$], **3**) (Scheme 2). We explored insertion both into the internal (CH_2) and terminal (CH_3) positions of propane, which lead to insertion products **4** and **5**, respectively. Our model system closely resembles that employed in the seminal computational study of Nakamura and coworkers,[137] in which propane and the same catalyst model was used. However, they only explored acceptor diazo compounds and did not consider the effects axial ligand binding might have on reactivity and selectivity.

Scheme 2. Rh-catalyzed transformation of A/A, D/A, and D/D diazo compounds and propane to C–H insertion products.

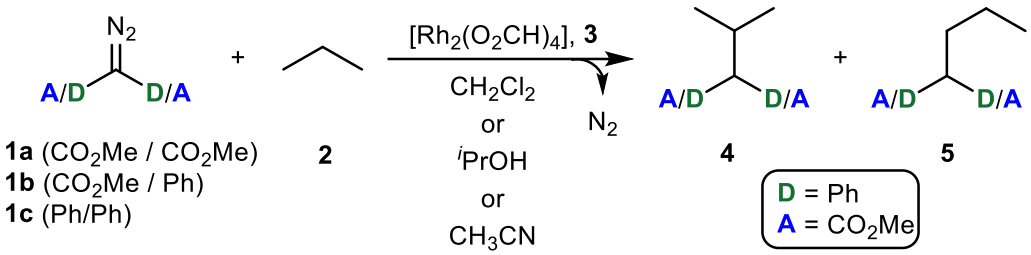

A schematic representation of the generally accepted mechanism for the C–H insertion process is shown in Figure 1 (blue inner ring). The reaction starts with nucleophilic attack of the diazo compound (**1**) on dirhodium tetraformate (**3**) to generate an ylide (**6**). Dirhodium carbene (**7**) is formed by N_2 extrusion from **6**. A weakly bound

complex (**8**) is then formed, from which the carbene carbon inserts into a C–H bond of propane (**2**). Such C–H insertions are generally concerted, but involve asynchronous formation of the new C–H and C–C bonds (with the former leading and the latter lagging).[137,138] However, Shaw and coworkers have found that donor/donor carbenes can undergo two-step, stepwise C–H insertions,[139] or exist at the borderlands[140] of concerted and stepwise.[141] Finally, dissociation of product **4** from weakly bound complex **9** regenerates catalyst **3**.

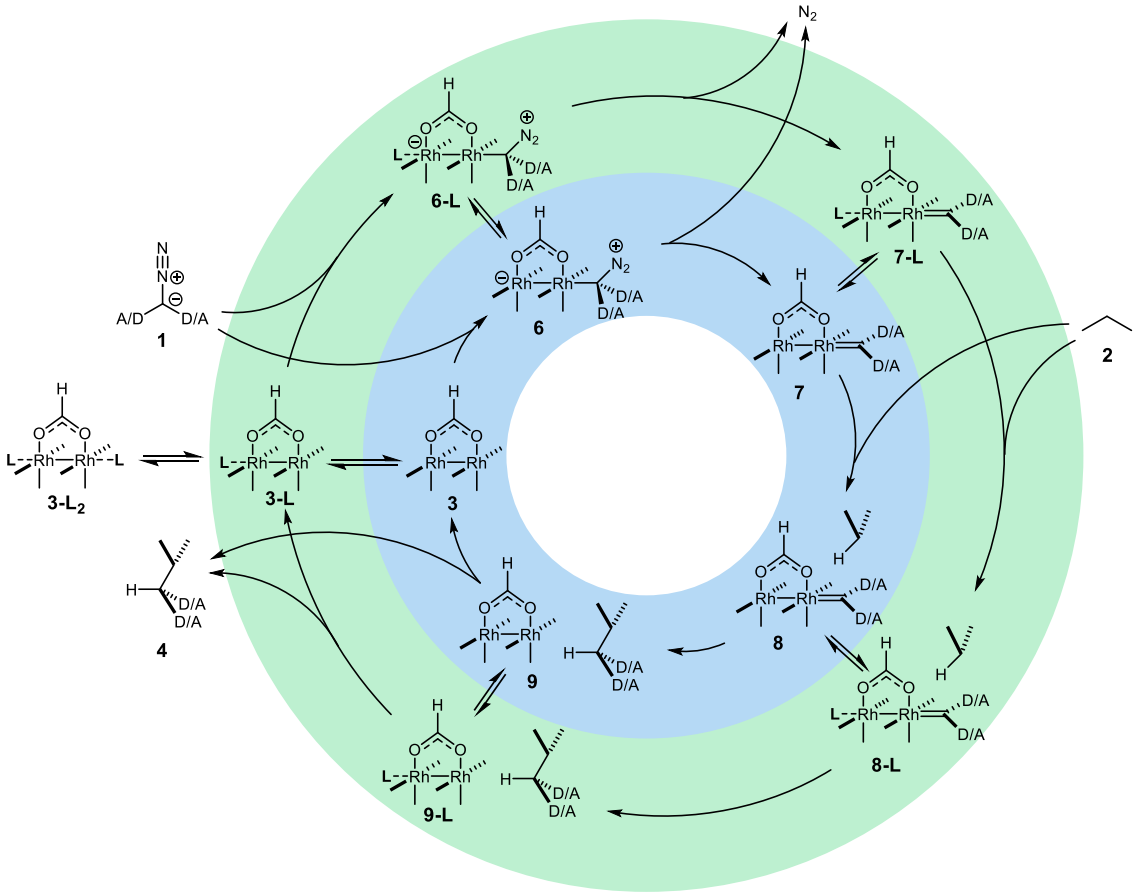

Figure 1. Mechanism postulated for the insertion of a diazo compound into propane catalyzed by dirhodium tetraformate (only one formate is shown explicitly). Blue inner ring: no axial ligand. Green outer ring: one axial ligand bound.

It is unclear whether axial solvent ligation is relevant at any point in this catalytic cycle (Figure 1, outer green circle versus inner blue circle). Solvent coordination may occur for some intermediates and not others (e.g., **3** to **3-L** equilibria) and when it coordinates, it may or may not have a significant effect on structure or reactivity. These issues are addressed below. Reactions with and without explicit coordinated solvent molecules were first studied in the gas-phase and then in three common solvents using the CPCM model: dichloromethane ($\varepsilon = 8.9$), isopropanol ($\varepsilon = 19.9$) and acetonitrile ($\varepsilon = 37.5$). We selected these solvents because they are commonly used in dirhodium catalyzed reactions, and because they provide variety of dielectric constants and donating ability.

Effects of solvent on diazo complexation: HOMO-LUMO modulation

To investigate the effects afforded by an axial ligand on diazo complexation, we assessed the frontier orbitals, the highest occupied molecular orbital (HOMO) and lowest unoccupied molecular orbital (LUMO), and their change in energetic splitting upon axial ligation. For this section, we narrow our attention on donor-acceptor (D/A) systems, a reasonable middle ground in terms of electrophilicity, selectivity, and functional group tolerance in the literature, but similar qualitative energetic trends were noted for D/D and A/A systems so the conclusions drawn from the D-A systems can reasonably be extended to those systems (see SI, Tables S1 and S2).[22]

Berry demonstrated that axial ligand coordination raises the energy of the Rh–Rh σ^* LUMO, and alters the HOMO-LUMO energy splitting.[55,58,59] An examination of the frontier orbitals of solvent-unbound [Rh_2(formate)$_4$] (**3**) and solvent-bound compounds **3-L** demonstrates that the LUMO energy increases by 1.3 eV (~ 30 kcal mol^{-1}) from **3** to **3-ACN**. While HOMO energies also increase, they do not increase by as much, and thus

the net effect is an increase in the HOMO-LUMO gap (by 0.62 eV from **3** to **3-ACN**; Figure 2). A similar effect is observed for dirhodium carbene structures **7** and **7-L**, but the magnitudes of the changes are much smaller than those observed with free [Rh_2(formate)$_4$] (Figure 3). Darko and coworkers computed similar qualitative trends in the HOMO-LUMO gap for their tethered, axial thioether-coordinated dirhodium catalysts with DFT calculations (M06-2X/def2TZVPP level of theory).[63] Increases to LUMO energies should lead to greater difficulty in forming **6**/**6-L**. The results of our computations support this notion.

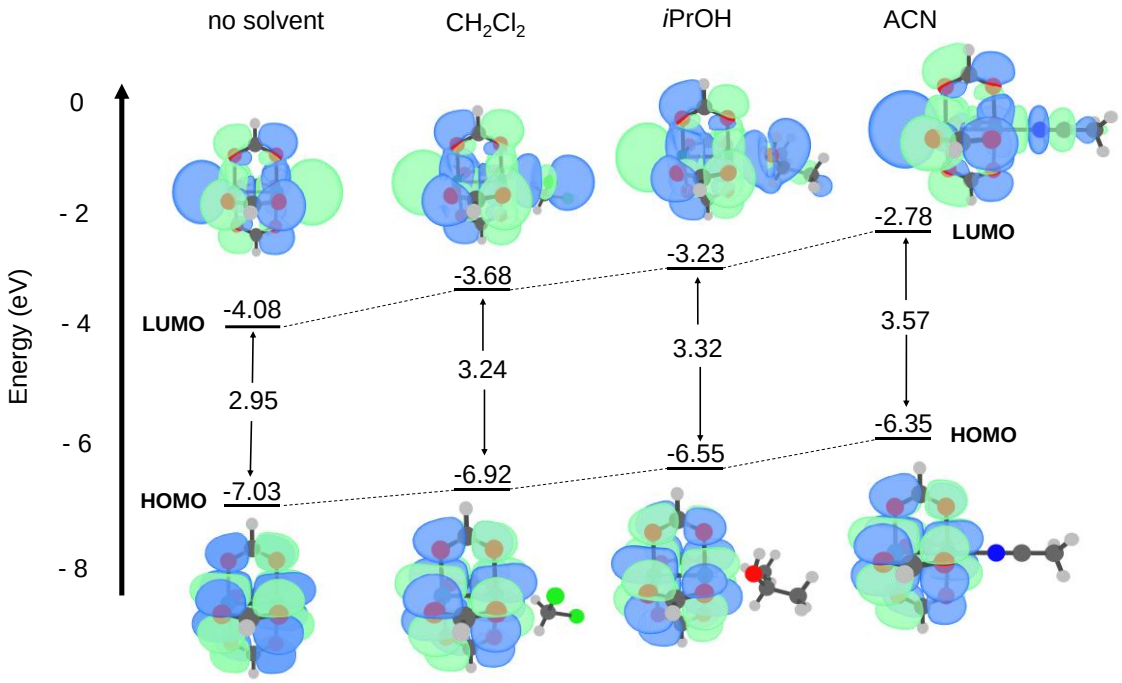

Figure 2. Frontier molecular orbitals (HOMO and LUMO) and HOMO-LUMO gaps (in eV) for **3** and **3-L** structures computed at the M06/SDD[6-311+G(d,p)]//B3LYP/LANL2DZ[6-31G(d)] level of theory.

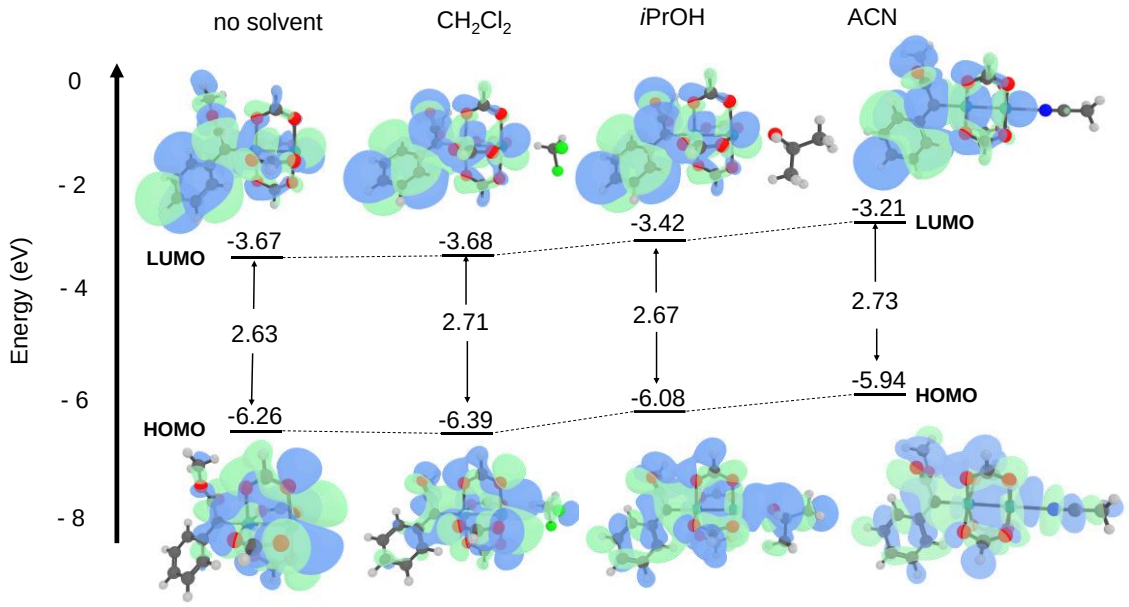

Figure 3. Frontier molecular orbitals (HOMO and LUMO) and HOMO-LUMO gaps (in eV) for **7** and **7-L** structures computed at the M06/SDD[6-311+G(d,p)]//B3LYP/LANL2DZ[6-31G(d)] level of theory.

Explicit versus implicit solvent – an acetonitrile case study

Next, we directed our attention towards whether including an explicit axial ligand changes predictions about mechanism and/or energetics compared to using an implicit solvent model. Of the three solvents studied, we expect acetonitrile to have the most significant effects on reactivity, since it is the strongest σ-donor,[53,55,60] so we focus on it here first.

Four approaches for modeling solvent were compared for the reaction of D/A diazo compound **1b** and propane to form C–H insertion products (Figure 4): (1) neither implicit nor explicit solvent included ("no coord. / gas"), (2) implicit solvent, but no explicit solvent included ("no coord. / acetonitrile"), (3) explicit solvent, but no implicit solvent included ("acetonitrile / gas"), (4) both implicit and explicit solvent included ("acetonitrile / acetonitrile"). Free energy barriers ($\Delta G^{\ddagger}$'s, relative to the minimum

immediately preceding the TSS in each case) for carbene formation and C–H insertion at both the CH_2 ("Internal") and CH_3 ("Terminal") positions of propane were computed using all four approaches. Free energy barriers varied within 3 kcal mol^{-1} for each reaction, a small change, but barriers for N_2 extrusion increased upon explicit solvent coordination and barriers for C–H insertion decreased upon solvent coordination to a lesser degree. *In summary, predicted effects are not large, but, if borne out in a flask, could alter rates by an order of magnitude or more.*

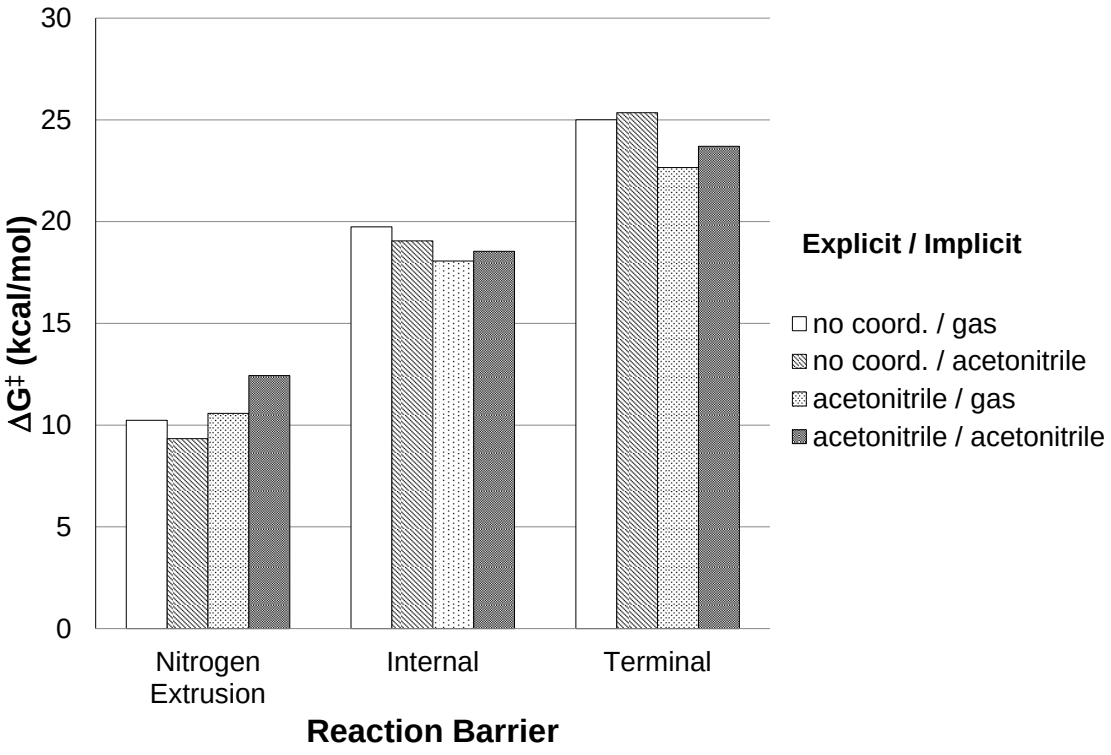

Figure 4. Variation of computed free energy barriers ($\Delta G^{‡}$) for N_2 extrusion (left), insertion at CH_2 internal position (center), and insertion at CH_3 terminal position (right) due to solvent model on donor-acceptor diazo compound (**1b**). All barriers are relative to the preceding minimum to each TSS.

Effects of solvent on N_2 extrusion barriers

Once it was clear that axial solvent coordination affected frontier molecular orbital energies of diazo complex (Figures 2 and 3) and energetic barriers (Figure 4), we proceeded to compare barriers for N_2 extrusion in other solvents (Figure 5). Here, all solvents are modeled with both implicit solvent and one explicit solvent molecule. Independent of carbene type, the barriers for N_2 extrusion increase with stronger σ-donor ligands. Of particular note is the absence of a barrier for the D/D system without a coordinated solvent – a caution for those modeling N_2 extrusion in such systems.

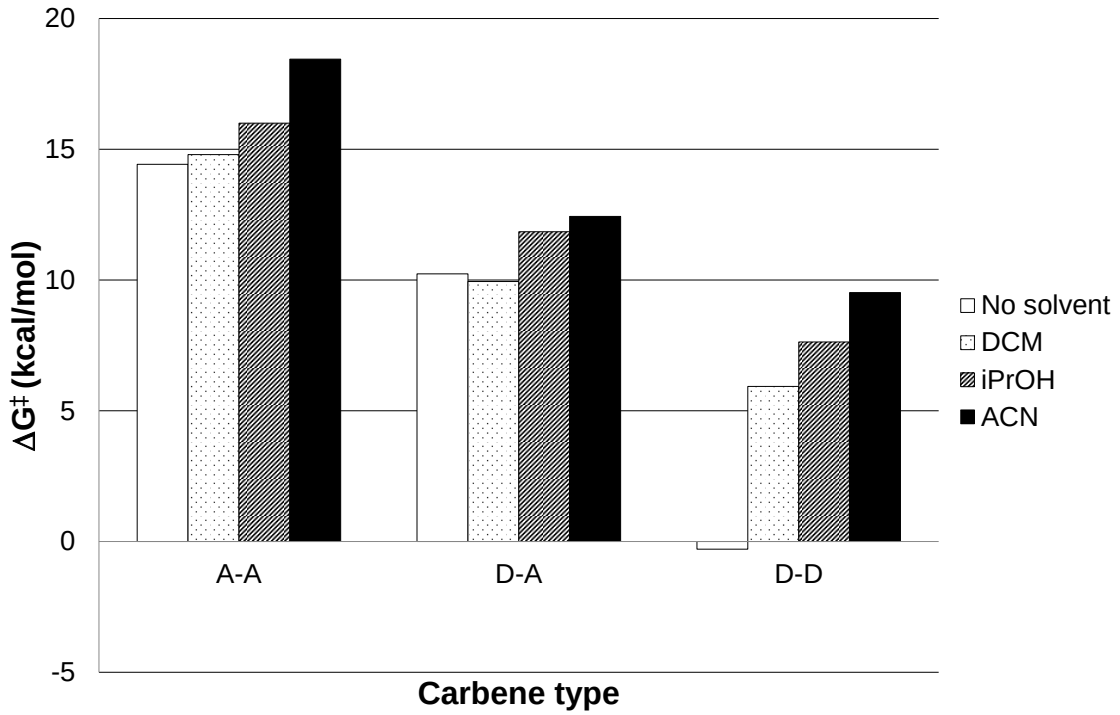

Figure 5. Comparison of the Gibbs free energy barriers of N_2 extrusion for acceptor/acceptor (A/A), donor/acceptor (D/A) and donor/donor (D/D) diazo compounds in gas-phase (No solvent) and dichloromethane (DCM), isopropanol (^{i}PrOH) and acetonitrile (ACN) solution. All barriers are relative to the preceding minimum to each TSS.

Gas-phase calculations with explicit solvent were used to isolate the effects of axial solvent on the N_2 extrusion barrier. Our results demonstrate that increasingly Lewis-basic axial ligands raise the energies of the (1) tetrahedral complex **6**/(**6-L**), (2) the N_2 extrusion TSS, and (3) dirhodium carbene **7**/(**7-L**) relative to the sum of the free energies of **1**-**3** (Figure 6). An increase in N_2 extrusion barriers (**6**/**6-L** → **7**/**7-L**) is observed for more strongly donating axial ligands; a similar qualitative trend is observed when implicit *and* explicit solvent are modeled (SI Figure S1). Why? Structures **6-*i*PrOH** and **6-ACN**, when optimized in the gas-phase from the endpoints of IRC paths originating from TSSs for N_2 extrusion, are not bound tetrahedral minima (Rh–C bonds are ~3.8 Å, C–N bonds are ~1.3 Å, and natural charges are redistributed); donation from the distal axial ligand appears to be sufficient to promote diazo dissociation., which, of course, hinders N_2 loss. As described by Fürstner and coworkers, Rh d-orbital back-bonding promotes N_2 extrusion and dirhodium carbene formation (Figure 6, inset),[45] an orbital interaction that is not fully expressed until the diazo carbon binds rhodium. The situation observed for **6-*i*PrOH** and **6-ACN** in the gas-phase is extreme, but a weaker version of the same effect is observed with any axial donor.

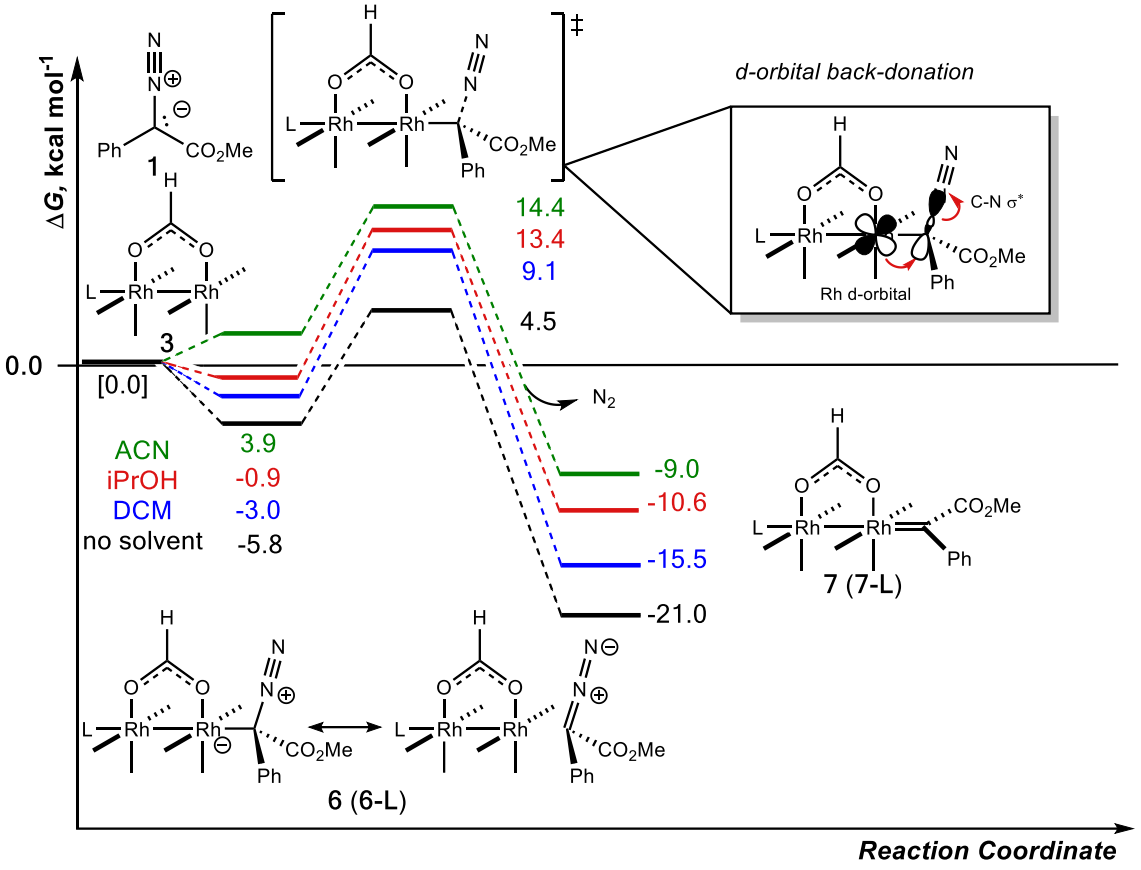

Figure 6. Formation and decomposition of **6**/**6-L** with and without solvent bound computed at the M06/SDD[6-311+G(d,p)]//B3LYP/LANL2DZ[6-31G(d)] level of theory for D/A diazo compounds (**1b**).

Effects of solvent on CH_2/CH_3 insertion selectivity

While the overall barriers for C–H insertion did not change much with solvent coordination, selectivity can be greatly affected by small changes in relative energies of transition states. The order of inherent reactivity for insertion into differently substituted alkyl C–H bonds is well-established—primary << secondary < tertiary C–H bonds—so we would expect our computed barriers for insertion into the internal position of propane to be lower than those for insertion into the terminal position.[137,142,143]

Kisan and Sunoj highlighted the effect that axial ligation can have on the selectivity of asymmetric N–H insertion reactions catalyzed by dirhodium tetracarboxylates with a chiral SPINOL-phosphoric acid bound.[88] In a similar manner, we can compute free energy differences ($\Delta\Delta G^{\ddagger}$) between transition states for insertion into internal versus terminal positions of propane. As shown in Figure 7, we computed synthetically meaningful differences in insertion barriers (see SI Figure S2 for $\Delta G^{\ddagger}$'s from which the $\Delta\Delta G^{\ddagger}$ are derived). For A/A carbenes, strongly donating solvents decrease selectivity. For D/A and D/D carbenes, however, *iso*-propanol coordination leads to the best selectivity (i.e., the greatest magnitude in $\Delta\Delta G^{\ddagger}$). Though we are unaware of experimental studies where *iso*-propanol leads to optimal selectivity, past studies show that selectivity can be solvent-dependent.[144] Given the magnitude of our predicted effects, decomposing their origins with current theoretical methods would not be reliable;[77,145] Nonetheless, Darko and co-workers observed an increase in product yield for Si–H insertion reactions when dirhodium catalysts with tethered, axial coordinating ligands were used.[63] Results in Figure 7 suggest that perhaps tethered, axial coordinating ligands might also enhance regioselectivity.

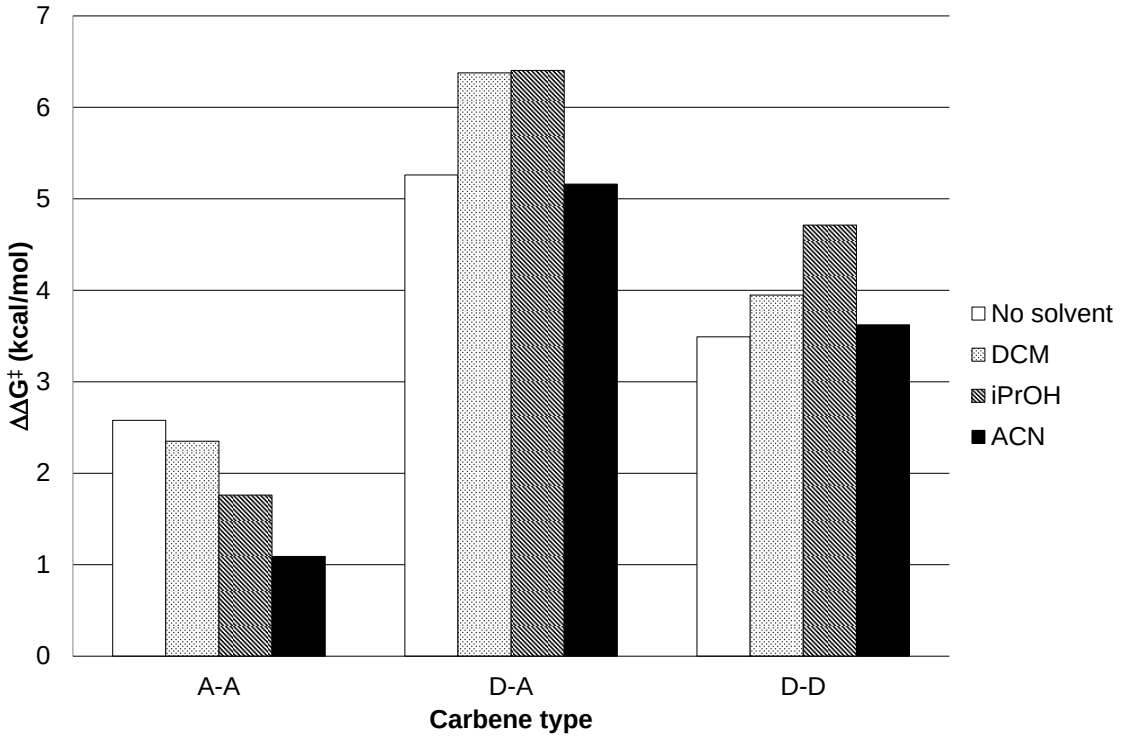

Figure 7. Comparison of the Gibbs free energy barriers difference for insertion of the carbene into the CH_2 and CH_3 of propane for acceptor/acceptor (A-A), donor/acceptor (D-A) and donor/donor (D-D) carbenes in gas phase and dichloromethane (DCM), isopropanol (^{i}PrOH) and acetonitrile (ACN) solution.

Structural changes upon axial ligand binding

How strong is the interaction between the axial ligand and the dirhodium complex? One classic, although debated,[146–148] means of characterizing bond strength is to use bond length as a measure for a series of related compounds. For the Rh–L interaction, where L is the atom of the axial solvent in contact with Rh, we compared d(Rh•••L) to the sum of the van der Waal radii of Rh and the bond atom of L ($\Sigma(r_{vdW})$), assuming a covalent interaction exists if d(Rh•••L) < $\Sigma(r_{vdW})$ (Scheme 3a).[149] We also computed Wiberg bond indices (WBIs)[150] for gas-phase geometries of **3**, **3-L**, **6**, **6-L**, **7**,

and **7-L**. These data are shown in Table 1. For all cases, *d*(Rh•••L) magnitudes are less than $\Sigma(r_{vdW})$, however WBIs for Rh–L bonds are low: 0.1-0.4. WBIs are greatest for acetonitrile, as expected, but similar for *iso*-propanol and dicholoromethane.

Scheme 3. a) key parameters collected in Table 1 b) representation of d_z^2 orbitals that contribute to the donor-acceptor interactions between Rh_2X_4 fragments that make up the Rh-Rh single bond c) orbital representation of donor-acceptor interaction and d) d-orbitals of Rh-Rh bond.

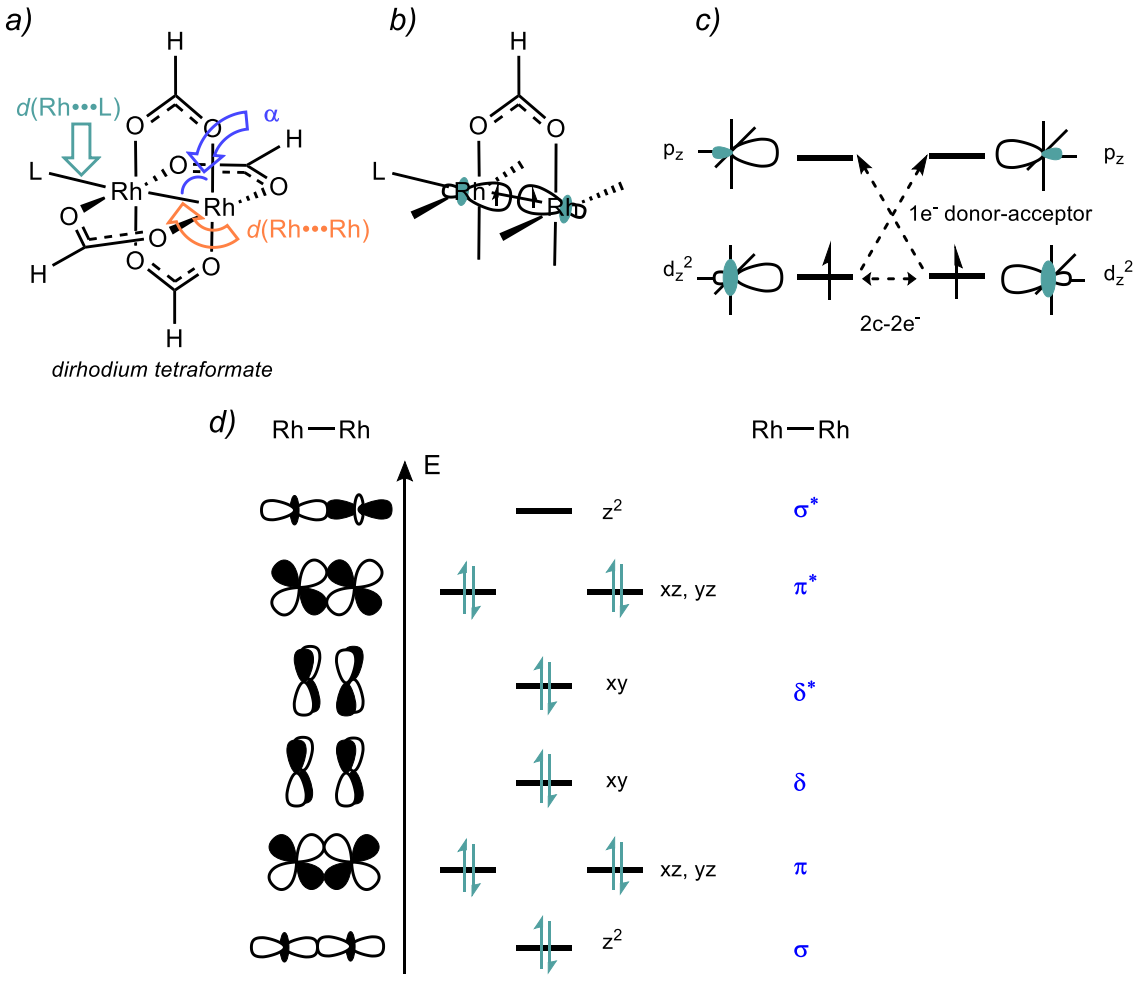

Table 1. Key distances (*d*(Rh•••Rh) and *d*(Rh•••L)), pyramidality angles (α), Wiberg bond indices (WBIs), and global electrophilicity index values (ω) for dirhodium complexes with axial ligands: DCM (L = Cl), ^{i}PrOH (L = O), and ACN (L = N). All complexes bound to diazo substrates are D-A substrates. Distance and orbital energies were measured from gas-phase M06/SDD[6-311+G(d,p)]//B3LYP/LANL2DZ[6-31G(d)] structures.

Rh_2 Complex	*d*(Rh•••Rh) (Å)	α	*d*(Rh•••L) (Å)	Rh-L $\Sigma(r_{vdW})$ (Å)[a]	Rh-Rh WBI	Rh-L WBI	ω (eV)
3	2.40	88.3	-	-	0.89	-	5.23
3-DCM	2.41	88.1	2.73	3.94	0.84	0.28	4.34
3-^{i}PrOH	2.42	88.2	2.27	4.26	0.83	0.23	3.59
3-ACN	2.43	88.2	2.20	4.10	0.81	0.36	2.91
6	2.43	88.0	-	-	0.77	-	3.82
6-DCM	2.43	87.7	2.84	3.94	0.78	0.23	3.59
6-^{i}PrOH	2.43	87.7	2.32	4.26	0.81	0.21	2.48
6-ACN	2.43	87.9	2.23	4.10	0.82	0.37	2.22
7	2.48	87.9	-	-	0.59	-	4.64
7-DCM	2.49	87.6	3.21	3.94	0.57	0.10	4.68
7-^{i}PrOH	2.49	87.7	2.51	4.26	0.64	0.14	4.23
7-ACN	2.49	87.5	2.49	4.10	0.63	0.23	3.84

Changes in Rh–Rh bond distances (*d*(Rh•••Rh)) are small with solvent coordination (Table 1). Pyramidality angle (α) (Scheme 3a) deviations from 90° are also small (Table 1), consistent with conclusions arrived at by Aullón and Alvarez.[151] While distortions of α might be expected since an axial ligand donates electron density into the Rh-Rh σ^* orbital, the bridging ligands, along with other orbital interactions, resist major deformation: (1) a 2c-2e$^-$ bond between the two d_z^2 orbitals of individual Rh_2X_4 fragments

and (2) a $1e^-$ donor-acceptor interaction between a d_z^2 of one Rh and the empty p_z of the other Rh (Scheme 3b and 3c).[55,151]

While small increases in *d*(Rh•••Rh) for **3**/**3-L** are accompanied by decreases in the Rh-Rh WBI, the Rh-L WBI increases in the series from no solvent to acetonitrile (Table 1). For **6**/**6-L** and **7**/**7-L**, changes in *d*(Rh•••Rh) (at most a 0.1 Å change) and Rh-Rh WBI are not as large (e.g., ΔWBI = 0.05 for **6-ACN** vs. ΔWBI = 0.08 for **3-ACN**), which suggests that the effects of axial solvent coordination on the Rh-Rh bond are not as potent compared to that of **3**. We suggest that the strong structural changes observed for **3**/**3-L** and diminished structural changes in **6**/**6-L** and **7**/**7-L** might be a result of a competition between L and the diazo compound to engage in 3c/4e bonding. Berry rationalized minor changes to the Rh-Rh bond distance upon axial complexation of increasing sigma-donor capacity in his 3c/4e bond model by observing that axial ligand binding mostly impacts the unoccupied LUMO orbital; in other words, the Rh-Rh bond length is generally insensitive to axial ligation.[58] The results in Table 1 for Rh-Rh distances that match crystallographically determined Rh-Rh bond distances (distances fall within a narrow window of ranging from 2.35-2.45 Å)[2,50,151]—and the minor, almost negligible, changes in WBIs—support this model.

Electrophilicity of the dirhodium core can be investigated by computing the global electrophilicity index (GEI, ω, equation 1,[66,152–155] wherein χ is electronegativity[156] and η is chemical hardness).[157] The GEI can be derived from HOMO and LUMO energies with equations 2 and 3.

$$\omega = \chi^2 / 2\eta \quad (1)$$

$$\chi = - (E_{HOMO} + E_{LUMO}) / 2 \quad (2)$$

$$\eta = E_{LUMO} - E_{HOMO} \quad (3)$$

Computed GEI values for **3/3-L**, **6**/**6-L**, and **7**/**7-L** (Table 1, the greater the value of ω, the greater the electrophilicity) suggest that axial ligation generally makes these structures less electrophilic and increasingly so from DCM to ACN, as one might expect.

SUMMARY AND OUTLOOK

In this study, we used DFT calculations to compute energetic barriers for N_2 extrusion and C–H insertion of A/A, D/A, and D/D carbenes with and without axial solvent ligation. Our attention centered around two main questions: (1) Is there a meaningful difference in reactivity and selectivity for such reactions when an implicit molecule is axially coordinated? (2) Is it possible to rationally tune reactivity and selectivity by solvent? In short, our study revealed that the answer to questions 1 and 2 are both "yes". While the predicted effects are not large, they are not negligible.

What do our results imply for future computational studies of dirhodium-catalyzed reactions, an increasingly important tool in aiding organic synthesis? We conclude that it is worth seriously considering axial solvent ligation in such studies. In some cases, the changes in relative energies will be small, in which case one can deduce that axial solvent might not play an important role; but in some cases, including axial solvent may be essential to accurately capture reactivity and selectivity—e.g., in computationally modeling stereoselective reactions,[158] in which case, accurately predicting $\Delta\Delta G^{\ddagger}$ may hinge on incorporating axial solvent in one's model—and missing the opportunity to do so due to axial solvent neglect would be an unfortunate oversight.

SUPPORTING INFORMATION

Supporting Data and Figures; Functionals and Basis Set Test; Energies and Frequencies.

A data set collection of computational results, including geometries and structure coordinates, is available in the ioChem-BD repository and can be accessed via https://doi.org/10.19061/iochem-bd-6-111

ACKNOWLEDGEMENTS

Support from the US National Science Foundation (CHE-1856416 and XSEDE) and the Ministerio de Educación, Cultura y Deporte, Programa Estatal de Promoción del Talento y su Empleabilidad en I+D+i, Subprograma Estatal de Movilidad del Plan Estatal de I+D+I (PRX19/00533) is gratefully acknowledged. We thank Prof. Jared T. Shaw (UC Davis) for encouragement, helpful discussion, and advice.

NOTES

The authors declare no competing financial interests.

REFERENCES

(1) Porai-Koshits, M. A.; Antsuskhima, A. S. The Structure of Rhodium Acetate Complexes. *Dokl. Akad. Nauk SSSR* **1962**, *146*, 1102–1105.

(2) Chifotides, H. T.; Dunbar, K. R. Rhodium Compounds. In *Multiple Bonds Between Metal Atoms*; Cotton, F. A., Murillo, C. A., Walton, R. A., Eds.; Springer: Boston, MA, 1982; pp 465–589.

(3) Hansen, J.; Davies, H. M. L. High Symmetry Dirhodium(II) Paddlewheel Complexes as Chiral Catalysts. *Coord. Chem. Rev.* **2008**, *252*, 545–555.

(4) Adly, F. G. On the Structure of Chiral Dirhodium(II) Carboxylate Catalysts: Stereoselectivity Relevance and Insights. *Catalysts* **2017**, *7*, 347.

(5) Berry, J. F.; Lu, C. C. Metal-Metal Bonds: From Fundamentals to Applications. *Inorg. Chem.* **2017**, *56*, 7577–7581.

(6) Farley, C. M.; Uyeda, C. Organic Reactions Enabled by Catalytically Active Metal–Metal Bonds. *Trends Chem.* **2019**, *1*, 497–509.

(7) Hrdina, R. Dirhodium(II,II) Paddlewheel Complexes. *Eur. J. Inorg. Chem.* **2021**, *2021*, 501–528.

(8) Abshire, A.; Moore, D.; Courtney, J.; Darko, A. Heteroleptic Dirhodium(II,II) Paddlewheel Complexes as Carbene Transfer Catalysts. *Org. Biomol. Chem.* **2021**, *19*, 8886–8905.

(9) Doyle, M. P. Electrophilic Metal Carbenes as Reaction Intermediates in Catalytic Reactions. *Acc. Chem. Res.* **1986**, *19*, 348–356.

(10) Doyle, M. P. Catalytic Methods for Metal Carbene Transformations. *Chem. Rev.* **1986**, *86*, 919–939.

(11) Chifotides, H. T.; Dunbar, K. R. Interactions of Metal-Metal-Bonded Antitumor Active Complexes with DNA Fragments and DNA. *Acc. Chem. Res.* **2005**, *38*, 146–156.

(12) Ohata, J.; Ball, Z. T. Rhodium at the Chemistry-Biology Interface. *Dalton Trans.* **2018**, *47*, 14855–14860.

(13) Sohrabi, M.; Saeedi, M.; Larijani, B.; Mahdavi, M. Recent Advances in Biological Activities of Rhodium Complexes: Their Applications in Drug Discovery Research. *Eur. J. Med. Chem.* **2021**, *216*, 113308.

(14) Cotton, F. A.; Lin, C.; Murillo, C. A. Supramolecular Arrays Based on Dimetal Building Units. *Acc. Chem. Res.* **2001**, *34*, 759–771.

(15) Reger, D. L.; Debreczeni, A.; Smith, M. D. Rhodium Paddlewheel Dimers Containing the π···π Stacking, 1,8-Naphthalimide Supramolecular Synthon. *Inorganica Chim. Acta* **2011**, *378*, 42–48.

(16) Furukawa, S.; Horike, N.; Kondo, M.; Hijikata, Y.; Carné-Sánchez, A.; Larpent, P.; Louvain, N.; Diring, S.; Sato, H.; Matsuda, R.; et al. Rhodium-Organic Cuboctahedra as Porous Solids with Strong Binding Sites. *Inorg. Chem.* **2016**, *55*, 10843–10846.

(17) Pirillo, J.; Hijikata, Y. Trans Influence across a Metal-Metal Bond of a Paddle-Wheel Unit on Interaction with Gases in a Metal-Organic Framework. *Inorg. Chem.* **2020**, *59*, 1193–1203.

(18) Padwa, A.; Weingarten, M. D. Cascade Processes of Metallo Carbenoids. *Chem. Rev.* **1996**, *96*, 223–269.

(19) Doyle, M. P.; Forbes, D. C. Recent Advances in Asymmetric Catalytic Metal Carbene Transformations. *Chem. Rev.* **1998**, *98*, 911–935.

(20) Doyle, M. P.; McKervey, M. A.; Ye, T. *Modern Catalytic Methods for Organic Synthesis with Diazo Compounds: From Cyclopropanes to Ylides*; Doyle, M. P., McKervey, M. A., Ye, T., Eds.; John Wiley & Sons, Inc.: New York, NY, 1998.

(21) Davies, H. M. L.; Manning, J. R. Catalytic C-H Functionalization by Metal

Carbenoid and Nitrenoid Insertion. *Nature* **2008**, *451*, 417–424.

(22) Davies, H. M. L.; Denton, J. R. Application of Donor/Acceptor-Carbenoids to the Synthesis of Natural Products. *Chem. Soc. Rev.* **2009**, *38*, 3061–3071.

(23) Davies, H. M. L.; Parr, B. T. Rhodium Carbenes. In *Contemporary Carbene Chemistry*; Moss, R. A., Doyle, M. P., Eds.; John Wiley & Sons, Inc., 2014; pp 363–403.

(24) Jana, S.; Guo, Y.; Koenigs, R. M. Recent Perspectives on Rearrangement Reactions of Ylides via Carbene Transfer Reactions. *Chem. Eur. J.* **2021**, *27*, 1270–1281.

(25) Zhu, D.; Chen, L.; Fan, H.; Yao, Q.; Zhu, S. Recent Progress on Donor and Donor–Donor Carbenes. *Chem. Soc. Rev.* **2020**, *49*, 908–950.

(26) Wei, B.; Sharland, J. C.; Lin, P.; Wilkerson-Hill, S. M.; Fullilove, F. A.; McKinnon, S.; Blackmond, D. G.; Davies, H. M. L. In Situ Kinetic Studies of Rh(II)-Catalyzed Asymmetric Cyclopropanation with Low Catalyst Loadings. *ACS Catal.* **2020**, *10*, 1161–1170.

(27) Bergstrom, B. D.; Nickerson, L. A.; Shaw, J. T.; Souza, L. W. Transition Metal Catalyzed Insertion Reactions with Donor/Donor Carbenes. *Angew. Chem. Int. Ed.* **2021**, *60*, 6864–6878.

(28) Davies, H. M. L.; Morton, D. Guiding Principles for Site Selective and Stereoselective Intermolecular C-H Functionalization by Donor/Acceptor Rhodium Carbenes. *Chem. Soc. Rev.* **2011**, *40*, 1857–1869.

(29) Davies, H. M. L.; Liao, K. Dirhodium Tetracarboxylates as Catalysts for Selective Intermolecular C–H Functionalization. *Nat. Rev. Chem.* **2019**, *3*, 347–

360.

(30) Adly, F. G.; Gardiner, M. G.; Ghanem, A. Design and Synthesis of Novel Chiral Dirhodium(II) Carboxylate Complexes for Asymmetric Cyclopropanation Reactions. *Chem. Eur. J.* **2016**, *22*, 3447–3461.

(31) Pirrung, M. C.; Liu, H.; Morehead, A. T. Rhodium Chemzymes: Michaelis-Menten Kinetics in Dirhodium(II) Carboxylate-Catalyzed Carbenoid Reactions. *J. Am. Chem. Soc.* **2002**, *124*, 1014–1023.

(32) Norman, J. G.; Kolari, H. J. Strength and Trans Influence of the Rh-Rh Bond in Rhodium(II) Carboxylate Dimers. *J. Am. Chem. Soc.* **1978**, *100*, 791–799.

(33) Christoph, G. G.; Koh, Y. B. Metal-Metal Bonding in Dirhodium Tetracarboxylates. Trans Influence and Dependence of the Rh-Rh Bond Distance upon the Nature of the Axial Ligands. *J. Am. Chem. Soc.* **1979**, *101*, 1422–1434.

(34) Aguirre, J. D.; Lutterman, D. A.; Angeles-Boza, A. M.; Dunbar, K. R.; Turro, C. Effect of Axial Coordination on the Electronic Structure and Biological Activity of Dirhodium(II,II) Complexes. *Inorg. Chem.* **2007**, *46*, 7494–7502.

(35) Liu, J.; Groszewicz, P. B.; Wen, Q.; Thankamony, A. S. L.; Zhang, B.; Kunz, U.; Sauer, G.; Xu, Y.; Gutmann, T.; Buntkowsky, G. Revealing Structure Reactivity Relationships in Heterogenized Dirhodium Catalysts by Solid-State NMR Techniques. *J. Phys. Chem. C* **2017**, *121*, 17409–17416.

(36) Pietruschka, D. S.; Kumari, B.; Buntkowsky, G.; Gutmann, T.; Mollenhauer, D. Mechanism of Heterogenization of Dirhodium Catalysts: Insights from DFT Calculations. *Inorg. Chem.* **2021**, *60*, 6239–6248.

(37) Nagashima, T.; Davies, H. M. L. Catalytic Asymmetric Cyclopropanation Using

Bridged Dirhodium Tetraprolinates on Solid Support. *Org. Lett.* **2002**, *4*, 1989–1992.

(38) Davies, H. M. L.; Walji, A. M. Asymmetric Intermolecular C-H Activation, Using Immobilized Dirhodium Tetrakis((S)-N-(Dodecylbenzenesulfonyl)-Prolinate) as a Recoverable Catalyst. *Org. Lett.* **2003**, *5*, 479–482.

(39) Davies, H. M. L.; Walji, A. M.; Nagashima, T. Simple Strategy for the Immobilization of Dirhodium Tetraprolinate Catalysts Using a Pyridine-Linked Solid Support. *J. Am. Chem. Soc.* **2004**, *126*, 4271–4280.

(40) Davies, H. M. L.; Walji, A. M. Universal Strategy for the Immobilization of Chiral Dirhodium Catalysts Huw. *Org. Lett.* **2005**, *7*, 2941–2944.

(41) Kataoka, Y.; Fukumoto, R.; Yano, N.; Atarashi, D.; Tanaka, H.; Kawamoto, T.; Handa, M. Synthesis, Characterization, Absorption Properties, and Electronic Structures of Paddlewheel-Type Dirhodium(II) Tetra-μ-(n-Naphthoate) Complexes: An Experimental and Theoretical Study. *Molecules* **2019**, *24*, 447.

(42) Fussell, E. D.; Darko, A. Adducts of Rhodium(II) Acetate and Rhodium(II) Pivalate with 1,8-Diazabicyclo[5.4.0]Undec-7-Ene. *Crystals* **2021**, *11*, 517.

(43) Das, A.; Wang, C.-H.; Van Trieste, G.; Sun, C.-J.; Chen, Y.-S.; Reibenspies, J.; Powers, D. In Crystallo Snapshots of Rh_2-Catalyzed C–H Amination. *J. Am. Chem. Soc.* **2020**, *142*, 19862–19867.

(44) Lu, W.; Zhu, X.; Yang, L.; Wu, X.; Xie, X.; Zhang, Z. Distinct Catalytic Performance of Dirhodium(II) Complexes with Ortho-Metalated DPPP in Dehydrosilylation of Styrene Derivatives with Alkoxysilanes. *ACS Catal.* **2021**, *11*, 10190–10197.

(45) Löffler, L. E.; Buchsteiner, M.; Collins, L. R.; Caló, F. P.; Singha, S.; Fürstner, A. $[Rh_2(MEPY)_4]$ and $[BiRh(MEPY)_4]$: Convenient Syntheses and Computational Analysis of Strikingly Dissimilar Siblings. *Helv. Chim. Acta* **2021**, *104*, e2100042.

(46) Wu, R.; Lu, J.; Cao, T.; Ma, J.; Chen, K.; Zhu, S. Enantioselective Rh(II)-Catalyzed Desymmetric Cycloisomerization of Diynes: Constructing Furan-Fused Dihydropiperidines with an Alkyne-Substituted Aza-Quaternary Stereocenter. *J. Am. Chem. Soc.* **2021**, *143*, 14916–14925.

(47) Vosáhlo, P.; Harmach, P.; Císařová, I.; Štěpnička, P. Synthesis and Characterisation of Dirhodium(II) Tetraacetates Bearing Axial Ferrocene Ligands. *J. Organomet. Chem.* **2021**, *953*, 122065.

(48) Cotton, F. A.; Hillard, E. A.; Murillo, C. A. The First Dirhodium Tetracarboxylate Molecule without Axial Ligation: New Insight into the Electronic Structures of Molecules with Importance in Catalysis and Other Reactions. *J. Am. Chem. Soc.* **2002**, *124*, 5658–5660.

(49) Werlé, C.; Goddard, R.; Fürstner, A. The First Crystal Structure of a Reactive Dirhodium Carbene Complex and a Versatile Method for the Preparation of Gold Carbenes by Rhodium-to-Gold Transmetalation. *Angew. Chem. Int. Ed.* **2015**, *54*, 15452–15456.

(50) Werlé, C.; Goddard, R.; Philipps, P.; Farès, C.; Fürstner, A. Structures of Reactive Donor/Acceptor and Donor/Donor Rhodium Carbenes in the Solid State and Their Implications for Catalysis. *J. Am. Chem. Soc.* **2016**, *138*, 3797–3805.

(51) Drago, R. S.; Tanner, S. P.; Richman, R. M.; Long, J. R. Quantitative Studies of Chemical Reactivity of Tetra-y-Butyrato-Dirhodium(II) Complexes. *J. Am.*

Chem. Soc. **1979**, *101*, 2897–2903.

(52) Drago, R. S.; Long, J. R.; Cosmano, R. Metal Synergism in the Coordination Chemistry of a Metal-Metal Bonded System: $Rh_2(C_3H_7COO)_4$. *Inorg. Chem.* **1981**, *20*, 2920–2927.

(53) Drago, R. S.; Long, J. R.; Cosmano, R. Comparison of the Coordination Chemistry and Inductive Transfer through the Metal—Metal Bond in Adducts of Dirhodium and Dimolybdenum Carboxylates. *Inorg. Chem.* **1982**, *21*, 2196–2202.

(54) Trindade, A. F.; Coelho, J. A. S. T.; Afonso, C. A. M.; Veiros, L. F.; Gois, P. M. P. Fine Tuning of Dirhodium(II) Complexes: Exploring the Axial Modification. *ACS Catal.* **2012**, *2*, 370–383.

(55) Warzecha, E.; Berto, T. C.; Berry, J. F. Axial Ligand Coordination to the C-H Amination Catalyst $Rh_2(esp)_2$: A Structural and Spectroscopic Study. *Inorg. Chem.* **2015**, *54*, 8817–8824.

(56) Johnson, S. A.; Hunt, H. R.; Neumann, H. M. Preparation and Properties of Anhydrous Rhodium(II) Acetate and Some Adducts Thereof. *Inorg. Chem.* **1963**, *2*, 960–962.

(57) Antos, J. M.; McFarland, J. M.; Iavarone, A. T.; Francis, M. B. Chemoselective Tryptophan Labeling with Rhodium Carbenoids at Mild pH. *J. Am. Chem. Soc.* **2009**, *131*, 6301–6308.

(58) Berry, J. F. The Role of Three-Center/Four-Electron Bonds in Superelectrophilic Dirhodium Carbene and Nitrene Catalytic Intermediates. *Dalton Trans.* **2012**, *41*, 700–713.

(59) Warzecha, E.; Berto, T. C.; Wilkinson, C. C.; Berry, J. F. Rhodium Rainbow: A Colorful Laboratory Experiment Highlighting Ligand Field Effects of Dirhodium Tetraacetate. *J. Chem. Educ.* **2019**, *96*, 571–576.

(60) Caló, F. P.; Bistoni, G.; Auer, A. A.; Leutzsch, M.; Fürstner, A. Triple Resonance Experiments for the Rapid Detection of ^{103}Rh NMR Shifts: A Combined Experimental and Theoretical Study into Dirhodium and Bismuth−Rhodium Paddlewheel Complexes. *J. Am. Chem. Soc.* **2021**, *143*, 12473–12479.

(61) Sarkar, M.; Daw, P.; Ghatak, T.; Bera, J. K. Amide-Functionalized Naphthyridines on a RhII –RhII Platform: Effect of Steric Crowding, Hemilability, and Hydrogen-Bonding Interactions on the Structural Diversity and Catalytic Activity of Dirhodium(II) Complexes. *Chem. Eur. J.* **2014**, *20*, 16537–16549.

(62) Sambasivan, R.; Zheng, W.; Burya, S. J.; Popp, B. V.; Turro, C.; Clementi, C.; Ball, Z. T. A Tripodal Peptide Ligand for Asymmetric Rh(II) Catalysis Highlights Unique Features of on-Bead Catalyst Development. *Chem. Sci.* **2014**, *5*, 1401–1407.

(63) Sheffield, W.; Abshire, A.; Darko, A. Effect of Tethered, Axial Thioether Coordination on Rhodium(II)-Catalyzed Silyl-Hydrogen Insertion. *Eur. J. Org. Chem.* **2019**, *2019*, 6347–6351.

(64) Cressy, D.; Zavala, C.; Abshire, A.; Sheffield, W.; Darko, A. Tuning Rh(II)-Catalysed Cyclopropanation with Tethered Thioether Ligands. *Dalton Trans.* **2020**, *49*, 15779–15787.

(65) Cressy, D. *Fine Tuning RhII Complexes with Tethered, Axial Coordination: Structural Studies and Application to Diazo-Mediated Cyclopropanation*

Reactions. PhD Diss., University of Tennessee; 2021.

(66) Ohnishi, R.; Ohta, H.; Mori, S.; Hayashi, M. Cationic Dirhodium Complexes Bridged by 2-Phosphinopyridines Having an Exquisitely Positioned Axial Shielding Group: A Molecular Design for Enhancing the Catalytic Activity of the Dirhodium Core. *Organometallics* **2021**, *40*, 2678–2690.

(67) Snyder, J. P.; Padwa, A.; Stengel, T.; Arduengo III, A. J.; Jockisch, A.; Kim, H.-J. A Stable Dirhodium Tetracarboxylate Carbenoid: Crystal Structure, Bonding Analysis, and Catalysis. *J. Am. Chem. Soc.* **2001**, *123*, 11318–11319.

(68) Gomes, L. F. R.; Trindade, A. F.; Candeias, N. R.; Veiros, L. F.; Gois, P. M. P.; Afonso, C. A. M. Cyclization of Diazoacetamides Catalyzed by N-Heterocyclic Carbene Dirhodium(II). *Synthesis* **2009**, *20*, 3519–3526.

(69) Anderson, B. G.; Cressy, D.; Patel, J. J.; Harris, C. F.; Yap, G. P. A.; Berry, J. F.; Darko, A. Synthesis and Catalytic Properties of Dirhodium Paddlewheel Complexes with Tethered, Axially Coordinating Thioether Ligands. *Inorg. Chem.* **2019**, *58*, 1728–1732.

(70) Xu, X.; Zavalij, P. Y.; Doyle, M. P. Catalytic Asymmetric Syntheses of Quinolizidines by Dirhodium-Catalyzed Dearomatization of Isoquinolinium/Pyridinium Methylides−The Role of Catalyst and Carbene Source. *J. Am. Chem. Soc.* **2013**, *135*, 12439–12447.

(71) Nelson, T. D.; Song, Z. J.; Thompson, A. S.; Zhao, M.; DeMarco, A.; Reamer, R. A.; Huntington, M. F.; Grabowski, E. J. J.; Reider, P. J. Rhodium-Carbenoid-Mediated Intermolecular O–H Insertion Reactions: A Dramatic Additive Effect. Application in the Synthesis of an Ascomycin Derivative. *Tetrahedron Lett.* **2000**, *41*, 1877–1881.

(72) Marcoux, D.; Azzi, S.; Charette, A. B. $TfNH_2$ as Achiral Hydrogen-Bond Donor Additive to Enhance the Selectivity of a Transition Metal Catalyzed Reaction. Highly Enantio- And Diastereoselective Rhodium-Catalyzed Cyclopropanation of Alkenes Using α-Cyano Diazoacetamide. *J. Am. Chem. Soc.* **2009**, *131*, 6970–6972.

(73) Marcoux, D.; Lindsay, V. N. G.; Charette, A. B. Use of Achiral Additives to Increase the Stereoselectivity in Rh(II)-Catalyzed Cyclopropanations. *Chem. Commun.* **2010**, *46*, 910–912.

(74) Lindsay, V. N. G.; Nicolas, C.; Charette, A. B. Asymmetric Rh(II)-Catalyzed Cyclopropanation of Alkenes with Diacceptor Diazo Compounds: P-Methoxyphenyl Ketone as a General Stereoselectivity Controlling Group. *J. Am. Chem. Soc.* **2011**, *133*, 8972–8981.

(75) Sharland, J. C.; Wei, B.; Hardee, D. J.; Hodges, T. R.; Gong, W.; Voight, E. A.; Davies, H. M. L. Role of Additives to Overcome Limitations of Intermolecular Rhodium-Catalyzed Asymmetric Cyclopropanation. *ChemRxiv* **2021**, doi: 10.26434/chemrxiv.14479593.v1.

(76) Varghese, J. J.; Mushrif, S. H. Origins of Complex Solvent Effects on Chemical Reactivity and Computational Tools to Investigate Them: A Review. *React. Chem. Eng.* **2019**, *4*, 165–206.

(77) Wynne, D. C.; Olmstead, M. M.; Jessop, P. G. Supercritical and Liquid Solvent Effects on the Enantioselectivity of Asymmetric Cyclopropanation with Tetrakis[1-[(4-Tert-Butylphenyl)- Sulfonyl]-(2S)-Pyrrolidinecarboxylate]Dirhodium(II). *J. Am. Chem. Soc.* **2000**, *122*, 7638–7647.

(78) Rosales, A.; Rodríguez-García, I.; López-Sánchez, C.; Álvarez-Corral, M.;

Muñoz-Dorado, M. Solvent Influence in the Rh-Catalyzed Intramolecular 1,6 C-H Insertions: A General Approach to the Chromane and Flavanone Skeletons. *Tetrahedron* **2011**, *67*, 3071–3075.

(79) Yang, Z.; Guo, Y.; Koenigs, R. M. Solvent-Dependent, Rhodium Catalysed Rearrangement Reactions of Sulfur Ylides. *Chem. Commun.* **2019**, *55*, 8410–8413.

(80) Candeias, N. R.; Gois, P. M. P.; Afonso, C. A. M. Rh(II) Catalysed Intramolecular C-H Insertion of Diazo Substrates in Water: A Simple and Efficient Approach to Catalyst Reuse. *Chem. Commun.* **2005**, 391–393.

(81) Candeias, N. R.; Gois, P. M. P.; Afonso, C. A. M. Rh(II)-Catalyzed Intramolecular C-H Insertion of Diazo Substrates in Water: Scope and Limitations. *J. Org. Chem.* **2006**, *71*, 5489–5497.

(82) Wurz, R. P.; Charette, A. B. Transition Metal-Catalyzed Cyclopropanation of Alkenes in Water: Catalyst Efficiency and in Situ Generation of the Diazo Reagent. *Org. Lett.* **2002**, *4*, 4531–4533.

(83) Zhu, C.-Z.; Wei, Y.; Shi, M. Rhodium(II)-Catalyzed Intramolecular Transannulation of 4-Methoxycyclohexa-2,5-Dienone Tethered 1-Sulfonyl-1,2,3-Triazoles: Synthesis of Azaspiro[5.5]Undecane Derivatives. *Adv. Synth. Catal.* **2019**, *361*, 3430–3435.

(84) Zhu, C.-Z.; Wei, Y.; Shi, M. Rhodium(II)-Catalyzed Divergent Intramolecular Tandem Cyclization of N-or O-Tethered Cyclohexa-2,5-Dienones with 1-Sulfonyl-1,2,3- Triazole: Synthesis of Cyclopropa[Cd]Indole and Benzofuran Derivatives. *Org. Chem. Front.* **2019**, *6*, 2884–2891.

(85) Nickerson, L. A.; Bergstrom, B. D.; Gao, M.; Shiue, Y. S.; Laconsay, C. J.; Culberson, M. R.; Knauss, W. A.; Fettinger, J. C.; Tantillo, D. J.; Shaw, J. T. Enantioselective Synthesis of Isochromans and Tetrahydroisoquinolines by C-H Insertion of Donor/Donor Carbenes. *Chem. Sci.* **2020**, *11*, 494–498.

(86) Chiappini, N. D.; Mack, J. B. C.; Du Bois, J. Intermolecular C(sp^3)−H Amination of Complex Molecules. *Angew. Chem. Int. Ed.* **2018**, *57*, 4956–4959.

(87) Hansen, J.; Li, B.; Dikarev, E.; Autschbach, J.; Davies, H. M. L. Combined Experimental and Computational Studies of Heterobimetallic Bi-Rh Paddlewheel Carboxylates as Catalysts for Metal Carbenoid Transformations. *J. Org. Chem.* **2009**, *74*, 6564–6571.

(88) Kisan, H. K.; Sunoj, R. B. Axial Coordination Dichotomy in Dirhodium Carbenoid Catalysis: A Curious Case of Cooperative Asymmetric Dual-Catalytic Approach toward Amino Esters. *J. Org. Chem.* **2015**, *80*, 2192–2197.

(89) Mato, M.; Montesinos-Magraner, M.; Sugranyes, A. R.; Echavarren, A. M. Rh(II)-Catalyzed Alkynylcyclopropanation of Alkenes by Decarbenation of Alkynylcycloheptatrienes. *J. Am. Chem. Soc.* **2021**, *143*, 10760–10769.

(90) Li, F.; Pei, C.; Koenigs, R. M. Rhodium-Catalyzed Cascade Reactions of Triazoles with Organoselenium Compounds – A Combined Experimental and Mechanistic Study. *Chem. Sci.* **2021**, *12*, 6362–6369.

(91) Zhao, Y.-T.; Su, Y.-X.; Li, X.-Y.; Yang, L.-L.; Huang, M.-Y.; Zhu, S.-F. Dirhodium-Catalyzed Enantioselective B–H Bond Insertion of Gem-Diaryl Carbenes: Efficient Access to Gem-Diarylmethine Boranes. *Angew. Chem. Int. Ed.* **2021**, *60*, 24214–24219.

(92) Harrison, J. G.; Gutierrez, O.; Jana, N.; Driver, T. G.; Tantillo, D. J. Mechanism of Rh2(II)-Catalyzed Indole Formation: The Catalyst Does Not Control Product Selectivity. *J. Am. Chem. Soc.* **2016**, *138*, 487–490.

(93) Laconsay, C. J.; Tantillo, D. J. Metal Bound or Free Ylides as Reaction Intermediates in Metal-Catalyzed [2,3]-Sigmatropic Rearrangements? It Depends. *ACS Catal.* **2021**, *11*, 829–839.

(94) Laconsay, C. J.; Tantillo, D. J. Melding of Experiment and Theory Illuminates Mechanisms of Metal-Catalyzed Rearrangements: Computational Approaches and Caveats. *Synthesis* **2021**, *53*, 3639–3652.

(95) Sperger, T.; Sanhueza, I. A.; Kalvet, I.; Schoenebeck, F. Computational Studies of Synthetically Relevant Homogeneous Organometallic Catalysis Involving Ni, Pd, Ir, and Rh: An Overview of Commonly Employed DFT Methods and Mechanistic Insights. *Chem. Rev.* **2015**, *115*, 9532–9586.

(96) Sperger, T.; Sanhueza, I. A.; Schoenebeck, F. Computation and Experiment: A Powerful Combination to Understand and Predict Reactivities. *Acc. Chem. Res.* **2016**, *49*, 1311–1319.

(97) Ryu, H.; Park, J.; Kim, H. K.; Park, J. Y.; Kim, S.-T.; Baik, M.-H. Pitfalls in Computational Modeling of Chemical Reactions and How To Avoid Them. *Organometallics* **2018**, *37*, 3228–3239.

(98) Ahn, S.; Hong, M.; Sundararajan, M.; Ess, D. H.; Baik, M.-H. Design and Optimization of Catalysts Based on Mechanistic Insights Derived from Quantum Chemical Reaction Modeling. *Chem. Rev.* **2019**, *119*, 6509–6560.

(99) Harvey, J. N.; Himo, F.; Maseras, F.; Perrin, L. Scope and Challenge of

Computational Methods for Studying Mechanism and Reactivity in Homogeneous Catalysis. *ACS Catal.* **2019**, *9*, 6803–6813.

(100) Eisenstein, O.; Ujaque, G.; Lledós, A. What Makes a Good (Computed) Energy Profile? In *New Directions in the Modeling of Organometallic Reactions. Topics in Organometallic Chemistry*; Lledós, A., Ujaque, G., Eds.; Springer, 2020; Vol. 67, pp 1–38.

(101) Morgante, P.; Peverati, R. The Devil in the Details: A Tutorial Review on Some Undervalued Aspects of Density Functional Theory Calculations. *Int. J. Quantum Chem.* **2020**, *120*, e26332.

(102) Qi, X.; Lan, Y. Recent Advances in Theoretical Studies on Transition-Metal-Catalyzed Carbene Transformations. *Acc. Chem. Res.* **2021**, *54*, 2905–2915.

(103) Matsuzawa, A.; Harvey, J. N.; Himo, F. On the Importance of Considering Multinuclear Metal Sites in Homogeneous Catalysis Modeling. *Top. Catal.* **2021**, https://doi.org/10.1007/s11244-021-01507-z.

(104) Frisch, M. J.; Trucks, G. W.; Schlegel, H. B.; Scuseria, G. E. .; Robb, G. E.; Cheeseman, J. R.; Scalmani, G.; Barone, V.; Mennucci, B. .; Petersson, G. A.; Nakatsuji, H.; Caricato, M.; Li, X.; Hratchian, H. P. .; Izmaylov, A. F.; Bloino, J.; Zheng, G.; Sonnenberg, J. L.; Hada, M. .; Ehara, M.; Toyota, K.; Fukuda, R.; Hasegawa, J.; Ishida, M.; Nakajima, T. .; Honda, Y.; Kitao, O.; Nakai, H.; Vreven, T.; Montgomery, Jr., J. A. . P.; J. E.; Ogliaro, F.; Bearpark, M.; Heyd, J. J.; Brothers, E. . K.; K. N.; Staroverov, V. N.; Keith, T.; Kobayashi, R.; Normand, J. . R.; K.; Rendell, A.; Burant, J. C.; Iyengar, S. S.; Tomasi, J. . C.; M.; Rega, N.; Millam, J. M.; Klene, M.; Knox, J. E.; Cross, J. B. .; et al. Gaussian 09, Revision D.01. *Gaussian Inc.* Wallingford, CT 2009.

(105) Fukui, K. The Path of Chemical Reactions -- The IRC Approach. *Acc. Chem. Res.* **1981**, *14*, 363–368.

(106) Gonzalez, C.; Schlegel, H. B. Reaction Path Following In Mass-Weighted Internal Coordinates Cartesians and with Internal Coordinates without Mass-Weighting. *J. Phys. Chem.* **1990**, *94*, 5523–5527.

(107) Maeda, S.; Harabuchi, Y.; Ono, Y.; Taketsugu, T.; Morokuma, K. Intrinsic Reaction Coordinate: Calculation, Bifurcation, and Automated Search. *Int. J. Quantum Chem.* **2015**, *115*, 258–269.

(108) Becke, A. D. Density-Functional Thermochemistry. III. The Role of Exact Exchange. *J. Chem. Phys.* **1993**, *98*, 5648–5652.

(109) Hay, P. J.; Wadt, W. R. Ab Initio Effective Core Potentials for Molecular Calculations. Potentials for the Transition Metal Atoms Sc to Hg. *J. Chem. Phys.* **1985**, *82*, 270–283.

(110) Barone, V.; Cossi, M. Quantum Calculation of Molecular Energies and Energy Gradients in Solution by a Conductor Solvent Model. *J. Phys. Chem. A* **1998**, *102*, 1995–2001.

(111) Cossi, M.; Rega, N.; Scalmani, G.; Barone, V. Energies, Structures, and Electronic Properties of Molecules in Solution with the C-PCM Solvation Model. *J. Comput. Chem.* **2003**, *24*, 669–681.

(112) Takano, Y.; Houk, K. N. Benchmarking the Conductor-like Polarizable Continuum Model (CPCM) for Aqueous Solvation Free Energies of Neutral and Ionic Organic Molecules. *J. Chem. Theory Comput.* **2005**, *1*, 70–77.

(113) Zhao, Y.; Truhlar, D. G. The M06 Suite of Density Functionals for Main Group

Thermochemistry, Thermochemical Kinetics, Noncovalent Interactions, Excited States, and Transition Elements: Two New Functionals and Systematic Testing of Four M06-Class Functionals and 12 Other Function. *Theor. Chem. Acc.* **2008**, *120*, 215–241.

(114) Fuentealba, P.; Preuss, H.; Stoll, H.; Von Szentpály, L. A Proper Account of Core-Polarization with Pseudopotentials: Single Valence-Electron Alkali Compounds. *Chem. Phys. Lett.* **1982**, *89*, 418–422.

(115) Weinhold, F.; Carpenter, J. E. The Natural Bond Orbital Lewis Structure Concept for Molecules, Radicals, and Radical Ions. In *The Structure of Small Molecules and Ions*; Naaman, R., Vager, Z., Eds.; Springer: Boston, MA, 1988; pp 227–236.

(116) Foster, J. P.; Weinhold, F. Natural Hybrid Orbitals. *J. Am. Chem. Soc.* **1980**, *102*, 7211–7218.

(117) Weinhold, F.; Landis, C. R.; Glendening, E. D. What Is NBO Analysis and How Is It Useful? *Int. Rev. Phys. Chem.* **2016**, *35*, 399–440.

(118) Glendening, E. D.; Reed, A. E.; Carpenter, J. E.; Weinhold, F. NBO Version 3.1 Gaussian Inc. Pittsburgh 2003.

(119) Nowlan III, D. T.; Gregg, T. M.; Davies, H. M. L.; Singleton, D. A. Isotope Effects and the Nature of Selectivity in Rhodium-Catalyzed Cyclopropanations. *J. Am. Chem. Soc.* **2003**, *125*, 15902–15911.

(120) Kisan, H. K.; Sunoj, R. B. Deciphering the Origin of Cooperative Catalysis by Dirhodium Acetate and Chiral Spiro Phosphoric Acid in an Asymmetric Amination Reaction. *Chem. Commun.* **2014**, *50*, 14639–14642.

(121) Lee, M.; Ren, Z.; Musaev, D. G.; Davies, H. M. L. Rhodium-Stabilized Diarylcarbenes Behaving as Donor/Acceptor Carbenes. *ACS Catal.* **2020**, *10*, 6240–6247.

(122) Nair, V. N.; Kojasoy, V.; Laconsay, C. J.; Kong, W. Y.; Tantillo, D. J.; Tambar, U. K. Catalyst-Controlled Regiodivergence in Rearrangements of Indole-Based Onium Ylide. *J. Am. Chem. Soc.* **2021**, *143*, 9016–9025.

(123) Kozuch, S.; Shaik, S. How to Conceptualize Catalytic Cycles? The Energetic Span Model. *Acc. Chem. Res.* **2011**, *44*, 101–110.

(124) Anciaux, A. J.; Hubert, A. J.; Noels, A. F.; Petiniot, N.; Teyssié, P. Transition-Metal-Catalyzed Reactions of Diazo Compounds. 1. Cyclopropanation of Double Bonds. *J. Org. Chem.* **1980**, *45*, 695–702.

(125) Zhao, Y.; Truhlar, D. G. A New Local Density Functional for Main-Group Thermochemistry, Transition Metal Bonding, Thermochemical Kinetics, and Noncovalent Interactions. *J. Chem. Phys.* **2006**, *125*, 194101.

(126) Yu, H. S.; He, X.; Li, S. L.; Truhlar, D. G. MN15: A Kohn-Sham Global-Hybrid Exchange-Correlation Density Functional with Broad Accuracy for Multi-Reference and Single-Reference Systems and Noncovalent Interactions. *Chem. Sci.* **2016**, *7*, 5032–5051.

(127) Grimme, S.; Antony, J.; Ehrlich, S.; Krieg, H. A Consistent and Accurate Ab Initio Parametrization of Density Functional Dispersion Correction (DFT-D) for the 94 Elements H-Pu. *J. Chem. Phys.* **2010**, *132*, 154104.

(128) Grimme, S.; Ehrlich, S.; Goerigk, L. Effect of the Damping Function in Dispersion Corrected Density Functional Theory. *J. Comput. Chem.* **2011**, *32*,

1456–1465.

(129) Liao, K.; Pickel, T. C.; Boyarskikh, V.; Bacsa, J.; Musaev, D. G.; Davies, H. M. L. Site-Selective and Stereoselective Functionalization of Non-Activated Tertiary C-H Bonds. *Nature* **2017**, *551*, 609–613.

(130) Zhou, M.; Springborg, M. Theoretical Study of the Mechanism behind the Site- and Enantio-Selectivity of C-H Functionalization Catalysed by Chiral Dirhodium Catalyst. *Phys. Chem. Chem. Phys.* **2020**, *22*, 9561–9572.

(131) Álvarez-Moreno, M.; De Graaf, C.; López, N.; Maseras, F.; Poblet, J. M.; Bo, C. Managing the Computational Chemistry Big Data Problem: The ioChem-BD Platform. *J. Chem. Inf. Model.* **2015**, *55*, 95–103.

(132) Ford, A.; Miel, H.; Ring, A.; Slattery, C. N.; Maguire, A. R.; McKervey, M. A. Modern Organic Synthesis with α-Diazocarbonyl Compounds. *Chem. Rev.* **2015**, *115*, 9981–10080.

(133) Medvedev, J. J.; Nikolaev, V. A. Recent Advances in the Chemistry of Rh Carbenoids: Multicomponent Reactions of Diazocarbonyl Compounds. *Russ. Chem. Rev.* **2015**, *84*, 737–757.

(134) Davies, H. M. L.; Beckwith, R. E. J. Catalytic Enantioselective C-H Activation by Means of Metal-Carbenoid-Induced C-H Insertion. *Chem. Rev.* **2003**, *103*, 2861–2903.

(135) Staudinger, H.; Endle, R. Über Reaktionen Des Methylens. IV: Über Die Zersetzung Der Ketene Bei Hoher Temperatur. *Ber. Dtsch. Chem. Ges.* **1913**, *46*, 1437–1442.

(136) Shaw, J. T. C-H Insertion Reactions of Donor/Donor Carbenes: Inception,

Investigation, and Insights. *Synlett* **2020**, *31*, 838–844.

(137) Nakamura, E.; Yoshikai, N.; Yamanaka, M. Mechanism of C-H Bond Activation/C-C Bond Formation Reaction between Diazo Compound and Alkane Catalyzed by Dirhodium Tetracarboxylate. *J. Am. Chem. Soc.* **2002**, *124*, 7181–7192.

(138) Hare, S. R.; Tantillo, D. J. Cryptic Post-Transition State Bifurcations That Reduce the Efficiency of Lactone-Forming Rh-Carbenoid C-H Insertions. *Chem. Sci.* **2017**, *8*, 1442–1449.

(139) Lamb, K. N.; Squitieri, R. A.; Chintala, S. R.; Kwong, A. J.; Balmond, E. I.; Soldi, C.; Dmitrenko, O.; Castiñeira Reis, M.; Chung, R.; Addison, J. B.; et al. Synthesis of Benzodihydrofurans by Asymmetric C−H Insertion Reactions of Donor/Donor Rhodium Carbenes. *Chem. Eur. J.* **2017**, *23*, 11843–11855.

(140) Tantillo, D. J. Recent Excursions to the Borderlands between the Realms of Concerted and Stepwise: Carbocation Cascades in Natural Products Biosynthesis. *J. Phys. Org. Chem.* **2008**, *21*, 561–570.

(141) Dishman, S. N.; Laconsay, C. J.; Fettinger, J. C.; Tantillo, D. J.; Shaw, J. T. Divergent Stereochemical Outcomes in the Insertion of Donor/Donor Carbenes into the C–H Bonds of Stereogenic Centers. *ChemRxiv* **2021**, doi:10.33774/chemrxiv-2021-h06nc-v2.

(142) Taber, D. F.; Ruckle Jr., R. E. Cyclopentane Construction by $Rh_2(OAc)_4$-Mediated Intramolecular C-H Insertion: Steric and Electronic Effects. *J. Am. Chem. Soc.* **1986**, *108*, 7686–7693.

(143) Doyle, M. P.; Westrum, L. J.; Wolthuis, W. N. E.; See, M. M.; Boone, W. P.;

Bagheri, V.; Pearson, M. M. Electronic and Steric Control in Carbon-Hydrogen Insertion Reactions of Diazoacetoacetates Catalyzed by Dirhodium(II) Carboxylates and Carboxamides. *J. Am. Chem. Soc.* **1993**, *115*, 958–964.

(144) Zakrzewska, M. E.; Cal, P. M. S. D.; Candeias, N. R.; Bogel-Łukasik, R.; Afonso, C. A. M.; Ponte, M. N.; Gois, P. M. P. Intramolecular C–H Insertion Catalyzed by Dirhodium(II) Complexes Using CO_2 as the Reaction Media. *Green Chem. Lett. Rev.* **2012**, *5*, 211–240.

(145) Mu, L.; Drago, R. S.; Richardson, D. E. A Model Based QSPR Analysis of the Unified Non-Specific Solvent Polarity Scale. *J. Chem. Soc. Perkin Trans. 2* **1998**, *2*, 159–167.

(146) Badger, R. M. A Relation Between Internuclear Distances and Bond Force Constants. *J. Chem. Phys.* **1934**, *2*, 128–131.

(147) Huggins, M. L. Atomic Radii. IV. Dependence of Interatomic Distance on Bond Energy. *J. Am. Chem. Soc.* **1953**, *75*, 4126–4133.

(148) Kaupp, M.; Metz, B.; Stoll, H. Breakdown of Bond Length-Bond Strength Correlation: A Case Study. *Angew. Chem. Int. Ed.* **2000**, *39*, 4607–4609.

(149) Alvarez, S. A Cartography of the van Der Waals Territories. *Dalton Trans.* **2013**, *42*, 8617–8636.

(150) Wiberg, K. B. Application of the Pople-Santry-Segal CNDO Method to the Cyclopropylcarbinyl and Cyclobutyl Cation and to Bicyclobutane. *Tetrahedron* **1968**, *24*, 1083–1096.

(151) Aullón, G.; Alvarez, S. Pyramidality Effect on Rh(II)-Rh(II) Single Bonds. *Inorg. Chem.* **1993**, *32*, 3712–3719.

(152) Parr, R. G.; Szentpály, L. v.; Liu, S. Electrophilicity Index. *J. Am. Chem. Soc.* **1999**, *121*, 1922–1924.

(153) Chattaraj, P. K.; Sarkar, U.; Roy, D. R. Electrophilicity Index. *Chem. Rev.* **2006**, *106*, 2065–2091.

(154) Domingo, L. R.; Ríos-Gutiérrez, M.; Pérez, P. Applications of the Conceptual Density Functional Theory Indices to Organic Chemistry Reactivity. *Molecules* **2016**, *21*, 748.

(155) Jupp, A. R.; Johnstone, T. C.; Stephan, D. W. Improving the Global Electrophilicity Index (GEI) as a Measure of Lewis Acidity. *Inorg. Chem.* **2018**, *57*, 14764–14771.

(156) Parr, R. G.; Donnelly, R. A.; Levy, M.; Palke, W. E. Electronegativity: The Density Functional Viewpoint. *J. Chem. Phys.* **1978**, *68*, 3801–3807.

(157) Parr, R. G.; Pearson, R. G. Absolute Hardness: Companion Parameter to Absolute Electronegativity. *J. Am. Chem. Soc.* **1983**, *105*, 7512–7516.

(158) Peng, Q.; Duarte, F.; Paton, R. S. Computing Organic Stereoselectivity-from Concepts to Quantitative Calculations and Predictions. *Chem. Soc. Rev.* **2016**, *45*, 6093–6107.